



Article

Verifiable Surface Disinfection Using Ultraviolet Light with a Mobile Manipulation Robot †

Alan G. Sanchez *[‡] and William D. Smart *[‡]

Collaborative Robotics and Intelligent Systems (CoRIS) Institute, Oregon State University, Corvallis, OR 97330, USA

* Correspondence: sanchala@oregonstate.edu (A.G.S.); smartw@oregonstate.edu (W.D.S.)

† Presented at the 14th Pervasive Technologies Related to Assistive Environments Conference, Corfu, Greece, 29 June–2 July 2021.

‡ These authors contributed equally to this work.

Abstract: Robots are being increasingly used in the fight against highly-infectious diseases such as the Novel Coronavirus (SARS-CoV-2). By using robots in place of human health care workers in disinfection tasks, we can reduce the exposure of these workers to the virus and, as a result, often dramatically reduce their risk of infection. Since healthcare workers are often disproportionately affected by large-scale infectious disease outbreaks, this risk reduction can profoundly affect our ability to fight these outbreaks. Many robots currently available for disinfection, however, are little more than mobile platforms for ultraviolet lights, do not allow fine-grained control over how the disinfection is performed, and do not allow verification that it was done as the human supervisor intended. In this paper, we present a semi-autonomous system, originally designed for the disinfection of surfaces in the context of Ebola Virus Disease (EVD) that allows a human supervisor to direct an autonomous robot to disinfect contaminated surfaces to a desired level, and to subsequently verify that this disinfection has taken place. We describe the overall system, the user interface, how our calibration and modeling allows for reliable disinfection, and offer directions for future work to address open space disinfection tasks.

Keywords: UV disinfection robots; COVID-19; Ebola Virus Disease; coverage path planning



Citation: Sanchez, A.G.; Smart, W.D. Verifiable Surface Disinfection Using Ultraviolet Light with a Mobile Manipulation Robot. *Technologies* **2022**, *10*, 48. <https://doi.org/10.3390/technologies10020048>

Academic Editor: Fillia Makedon

Received: 30 December 2021

Accepted: 18 March 2022

Published: 29 March 2022

Publisher's Note: MDPI stays neutral with regard to jurisdictional claims in published maps and institutional affiliations.



Copyright: © 2022 by the authors. Licensee MDPI, Basel, Switzerland. This article is an open access article distributed under the terms and conditions of the Creative Commons Attribution (CC BY) license (<https://creativecommons.org/licenses/by/4.0/>).

1. Introduction

The novel Coronavirus (SARS-CoV-2), the cause of the global Coronavirus disease pandemic (COVID-19), has presented health risks worldwide, especially to health care workers [1]. The on-going global pandemic has stressed the healthcare infrastructure, often making it hard to care for providers to deliver an adequate standard of care to their patients. One approach that is being used to alleviate some of the immediate risks is to use semi-autonomous robots to disinfect surfaces and areas.

Typically, these robots are equipped with ultraviolet light (UV) sources, and are used to irradiate spaces in which Coronavirus may be present. If delivered at a suitable intensity, ultraviolet light inactivates the virus, rendering it safe. However, most systems that are currently available are little more than autonomous mobile robot bases with UV light tubes mounted on them. They are capable of navigating from place to place in a building, but rely on a human to tell them where to go, and when to turn the UV lights on. This leads the three possible shortcomings: (1) It is hard to determine when an area is suitably disinfected, since the system cannot determine when enough irradiation has been delivered; (2) A human operator might not choose the optimal position for the robot in a space, leading to poor disinfection quality due to shadows and occlusions; and (3) The system does not work well on horizontal surfaces, which receive much less irradiation than vertical walls, because of the geometry of the world.

In this paper, we describe a robot system that directly addresses these three problems, originally designed in the context of the Ebola Virus Disease (EVD). Our approach aims to reliably disinfect contaminated surfaces (fomites) to mitigate the risk of virus surface transmission, using a combination of human oversight and autonomous robotics. Our system can distance people from the actual disinfection work, reducing their overall risk of infection, reducing the need for personal protective equipment (PPE), and freeing up their time to work on more pressing duties. While reducing the risk of infection to health care workers is important, the on-going global COVID-19 pandemic has shown us that staff and PPE shortages are a significant problem in delivering a high quality of care [2].

Specifically, in this expanded version of our previous conference paper [3], we (1) give a brief overview of Ultraviolet Germicidal Irradiation (UVGI), and how it applies to viruses; (2) describe the design, implementation, and evaluation of a semi-autonomous robot system to perform UVGI on contaminated surfaces and how it relates to our prior work; (3) give details of our empirical modeling of an example ultraviolet light source, including how the actual performance deviates from the theoretically-expected one; and (4) offer directions for future work that will generalize our system to deal with open space disinfection, so that it is relevant to a wider range of pathogens.

2. Background

Before describing our system, we first give some background on the structure and transmission of viruses, to give the work more content and better understand how UV-based inactivation works. We then briefly introduce Ultraviolet Germicidal Irradiation modeling, which is an essential component of our system design.

2.1. Virus Structure and Transmission

A virus genome is a molecule made of either ribonucleic acid (RNA) or deoxyribonucleic acid (DNA). The capsid, a coat of protein molecules, protects the genome while also having a crucial role in binding and invading a host cell. When the virus is enveloped by a cell, the virus disassembles, and the viral genome gets transcribed and instructs the host cell to generate proteins for new viral capsids and molecules for viral genomes [4]. The replicated genomes and capsids reassemble, creating hundreds to thousands of viral particles [5]. These newly-formed viral particles burst through the host cell's outer membrane, damaging or destroying the host cell in search of new cells for viral replication. Thus, a person who contracts a virus becomes a reservoir of virus particles, which can be released through bodily secretions.

For example, virus transmission can occur through respiratory droplets, such as through a sneeze, cough, saliva, or mucus. A common transmission route into a person is via direct or indirect contact. Transmission from direct contact results when a person breathes in infected respiratory droplets from someone's cough or sneeze, whereas indirect contact occurs when they touch their nose, mouth, and eyes after touching an infected surface [6]. The Ebola virus is not an airborne virus and is spread mainly through direct contact of broken skin or mucus membranes with infected body fluids [7]. Due to the virus's transfer characteristics, the CDC recommends double impermeable gowns, eye protection, a hood, double gloves, and an N95 facemask for the minimum standard of PPE for suspected Ebola. However, the multi-layered PPE presented heat stress to healthcare workers when treating their patients [8]. In terms of COVID-19, the virus can spread both directly and indirectly. Doremalen et al. [9] investigated aerosol and surface stability of SARS-CoV-2, and the data revealed that the infected respiratory droplets can stay suspended in the air for up to three hours. The data also indicated that active COVID-19 was detected on stainless steel and plastic surfaces for up to 72 h.

2.2. UVGI Modeling

UVGI is an approach that utilizes UV light to inactivate a virus, which hampers the virus's ability to perform vital cellular functions for replication [10]. Virus inactivation

occurs because ultraviolet exposure results in damaging the nucleic acids. The UV light targets and disrupts the virus's genome and causes covalent bonds between adjacent uracil (in RNA) or adjacent thymine (in DNA) molecules. The abundant amount of covalent bonds lead to cellular mutations and prohibits a virus from reproducing [10,11]. UV light wavelengths between 200 and 290 nanometers (nm) have germicidal characteristics with the most effective wavelength range between 250–265 (nm) [10,12,13], which is within the UV-C band (200–280 nm).

Additionally, when on surfaces, viruses are more resilient than when suspended in the air [10,14]. The resistance increase has challenged researchers to accurately model surface ultraviolet germicidal irradiation. However, the database for UV rate constants for airborne viruses is a fair estimate for viruses on surfaces [10]. Knowing the UV rate constant of a virus is essential to model the decay rate for varying pathogens effectively.

Virus populations decay exponentially when exposed to UV light [10,15]. The first-order decay rate model for UV irradiation is expressed as

$$S = e^{-kD}, \quad (1)$$

where S is the survival fraction, which is the ratio of viruses before and after disinfection, k (m^2/J) is the UV rate constant, and D (J/m^2) is the UV exposure dose. The UV exposure dose is defined as

$$D = E_t \cdot I_r, \quad (2)$$

where I_r (W/m^2) is the irradiance, which is the radiative flux through a lit surface, and E_t (s) is the exposure time. A UV dose that provides 90% disinfection rate, also known as 10% Survival, is expressed as D_{90} . The irradiance, I_r is approximated by

$$I_r = \frac{\eta P}{A_{\text{exposed}}}, \quad (3)$$

where A_{exposed} is the exposed surface area, P is the source power rating, and η is the attenuation factor where $\eta \leq 1$. A conservative estimate of η is 0.1 [15].

3. Related Work

Robots have been widely used in the fight against COVID-19 in the on-going global pandemic. Yang et al. [16] provide an overview of the opportunities for robotics to mitigate the number of infectious disease outbreaks, while Cardona et al. [17] and Kaiser et al. [18] both briefly survey application areas for robots in the pandemic. Di Lallo et al. [19] give a survey of medical robot usage in the fight against infectious diseases, focusing on the use of robots across the continuum of care, from disease prevention to home care. They describe both the state of the practice (robots currently deployed) and the state of the art (research prototypes not yet widely deployed), and discuss challenges and required technologies for a wider use of robots in this setting. Courtney and Royal [20] survey the use of robots in the laboratory during the COVID-19 outbreak, focusing on the automation of existing processes to increase throughput and reduce risk for human technicians.

Shen et al. [21] provides a comprehensive survey of how robots were used in the first year of the COVID-19 pandemic. The survey covers both robots that were used directly in the fight against the disease and those that were used to provide continuity of operations in other areas of society. Of particular interest is the coverage of robots used for UV-C disinfection. Approximately ten systems are mentioned, both commercial and research, all having the same general morphology: vertically-mounted UV-C fluorescent tubes on a mobile base. The bases have varying amounts of autonomy, and are generally controlled by a human supervisor using a remote interface. None of the systems discussed in this paper are reported to have the ability to autonomously plan and execute the disinfection of a specified area.

One of the first mobile manipulation systems to be used for ultraviolet germicidal irradiation is the Agile Dexterous Autonomous Mobile Manipulation Robot (ADAMMS)

at the University of Southern California [22]. An existing manipulation robot platform is integrated into the system, and its manipulator holds a UV wand as its light source. The robot also requires a remote operator to control the wand's position across intricately shaped surfaces and objects. Limitations associated with this system are that the robot requires large amounts of teleoperation, there are no irradiation models provided from the teleoperated paths, and it relies on the human operator to achieve good coverage.

Tiseni et al. [23] report on a mobile disinfection robot that autonomously plans a trajectory using a Genetic Algorithm and a knowledge of the geometry of the space that it is in. The robot comprises a standard mobile base, with a number of UV-C lights, mounted vertically. Using UV-C sensitive markers, the effectiveness of a moving robot is compared to that of a static UV-C source in a typical indoor environment. The mobile system achieved better spatial coverage and provided more complete disinfection. Based on these findings, the authors propose a Genetic Algorithm (GA) based trajectory planner that attempts to find good trajectories through a known space to optimize the amount of UV-C radiation transmitted to surfaces. The algorithm uses an irradiation model and known room geometry to evaluate the GA fitness function, and was found to result in better trajectories after optimization, both in simulation and in the real world.

This work is most similar in spirit to our own. It addresses fomite disinfection, it attempts to measure the effectiveness of this infection empirically, and it uses an optimized trajectory to improve the delivery of UV-C radiation to the surfaces. In our setting, however, we can make assumptions about the surfaces to be disinfected, and we construct a reusable measurement system rather than using colorimetric markers. Our assumptions allow us to parameterize the optimization of our trajectory rather than to use a more general method like GAs, allowing us to plan in the higher-dimensional space of arm movements.

4. Prior Work

Our prior work [24] addressed modeling possible contamination in a simulated Ebola Treatment Unit (ETU) and dispatching a small mobile robot to clean it up. A field ETU is, essentially, a small tent with sleeping cots and basic medical equipment in it. The Ebola virus is hard to detect directly but, since it travels in bodily fluids, we can attempt to model the spread of these fluids in the ETU, and use this to model possible areas of contamination. Further, since these fluids do not generally move in their own, they must be tracked from one place to another by moving objects. For this work, we make the assumption that the only moving objects of significance are people walking about the ETU. Other moving objects are moved by people, so this assumption is a reasonable one, if we account for it in our modeling process.

We tracked the position of people moving in a small simulated ETU using a LiDAR mounted at approximately 1.5 m above the ground in a corner of the ETU. We filter the data from this LiDAR to remove static obstacles, spatially cluster the remaining data points using the DBSCAN algorithm [25], and fit ellipses to each of the clusters [26]. Since the LiDAR is mounted at the chest height of an average human, these ellipses form an approximate model of where people are in the ETU.

To track areas of possible contamination, we model the floor of the ETU as a grid, and keep a binary value (contaminated or not) in each grid cell. If a human moves from a contaminated cell to an uncontaminated one, we change the destination cell to be contaminated. We use the fitted ellipse to determine which cells the human is occupying for this calculation. It is worth noting that this is a very basic model of how contamination might move through the ETU. However, it is not an unreasonable one, and serves as a proof of concept of the general methodology.

To validate the modeling approach, we used fluorescent paint, which is easily detected when illuminated by ultraviolet light, and a calibrated video camera, as shown in Figure 1.



Figure 1. (Left): Tracking visualization. (Middle): Initial condition, showing paint. (Right): Final condition, showing paint under ultraviolet illumination.

An initial patch of paint, representing fluids contaminated with the Ebola virus, was placed near the bed in the ETU. A human moved around the ETU performing some fetch-and-carry tasks for a few minutes, while being tracked by the LiDAR system. We then compared the modeled contamination with the actual positions of the footprints made by the person, as shown in Figures 2 and 3.



Figure 2. (Left): Directly detected footprints (green) and modeled areas of contamination (grey) overlaid on the camera image of the ETU. (Right): Visualization of the tracked person and modeled contamination.

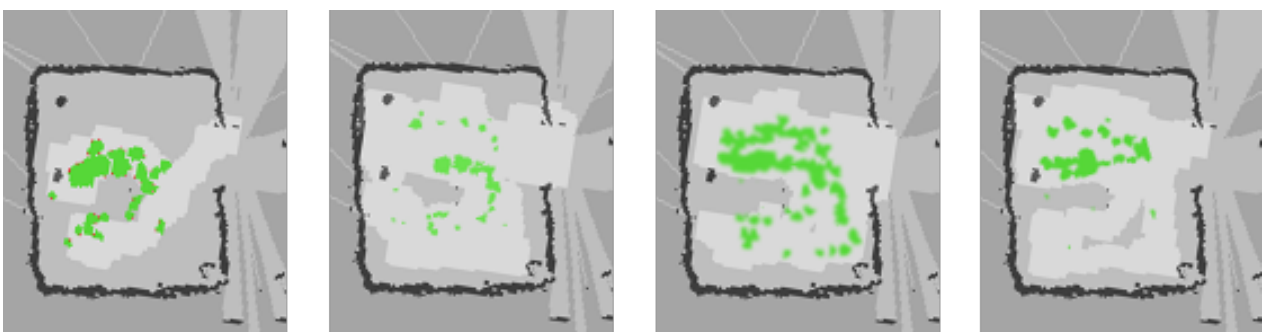


Figure 3. Directly detected footprints (green) overlaid with modeled areas of contamination (light grey).

As can be seen from the figures, the contamination modeling provides a conservative estimate of where there may be possible contamination.

Once we have an estimate of the contaminated areas of the floor, we dispatch a small mobile robot to decontaminate them. In a real-world deployment, this robot would be equipped with either a wet floor scrubber and a bleach-based solution or an ultraviolet light that would deactivate the virus present in the contaminated areas. As the robot

moves around the world, it changes the status of the model cells from contaminated to uncontaminated. A human supervisor can then look at a visualization of the space, to determine if all areas of possible contamination have been cleaned.

Relation to Current Work

Our prior work looked at Ebola contamination on the floor of an ETU, while our current work looks at surface disinfection using a mobile manipulation robot. While there are obvious similarities, such as the inactivation of a virus, there are also some less obvious connections. In both the prior and the current work, we cannot detect the contaminated areas directly. In the prior work, we make the reasonable assumption that the Ebola virus travels in bodily fluids and that these are only spread by people moving in the environment. In our current work, we rely on a human supervisor to determine where the possible contamination is.

In both systems, we model areas of possible contamination and use an autonomous robot to inactivate viruses in these areas. The robot uses the model to plan a path that will cover the contaminated areas, and autonomously executes this path. Both systems then present the results of the autonomous operation to a human supervisor for final approval. If the decontamination is not done correctly, the human can instruct the system to repeat the process, using an updated contamination model.

One of the key elements of both the prior and the current system is that we are using an autonomous robot to reduce the risk for humans by reducing the need for them to be near sources of potential contamination. However, we are not doing this fully autonomously, since this is neither practical nor prudent. In the real world, humans must remain in charge of high-consequence systems like these, for practical, ethical, and legal reasons. While we leverage autonomy as a key element of both systems, we wrap it in a layer of human supervision to provide the accountability that will be required if these systems are to be used in real deployments.

5. Surface Disinfection for Ebola Virus Disease

Previously mentioned in Section 3, Ebola is mainly transmitted through direct contact with an infected person's bodily fluids or through contact with a surface where these fluids are present [27], a process known as *fomite transmission*. Our prior work focused on surface disinfection to reduce the risk of these viral transmissions. Although previous work (see Section 3) gives many examples of UV-C disinfection robots, they are not well-suited to the disinfection of work surfaces. Many of these robots have vertically-mounted UV-C fluorescent light sources, which are inefficient for irradiating horizontal work surfaces. They also do not deal well with objects on these surfaces, which might cause shadows and a reduced amount of UV-C radiation reaching some areas of the surface [28]. Our system comprises a mobile manipulation robot (see Figure 4).

With a UV-C light source mounted on its end effector. The robot can maneuver the UV light source over the surface, ensuring a more complete and controlled irradiation. The system is semi-autonomous; a human supervisor designates the area to be disinfected and the level of disinfection required, then the robot plans and executes a series of arm movements to achieve this. The overall flow of operations is shown in Figure 5.

To operate the system, the human supervisor first teleoperates the mobile manipulator robot to a surface for disinfection. The robot is equipped with a depth camera and builds a voxel-based model of the surface (see Figure 6).



Figure 4. A Fetch robot hovering UV flashlight above UV sensor array.

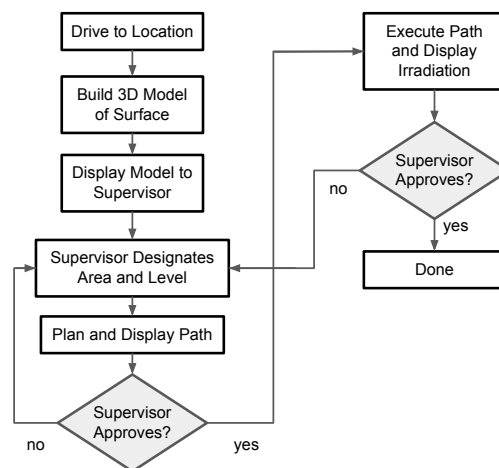


Figure 5. The flow of control in our system.

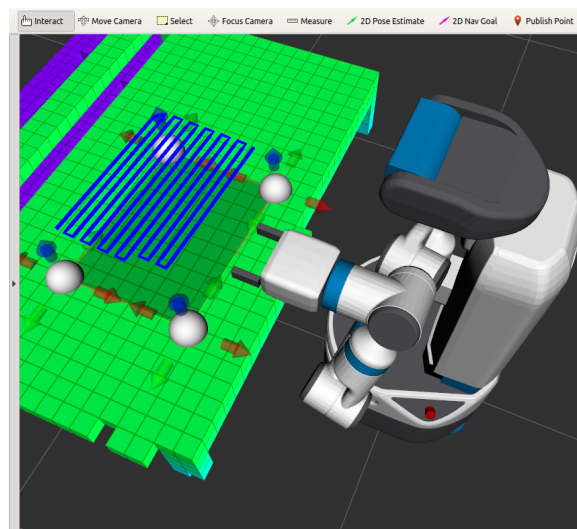


Figure 6. The 3D display interface. This is used to display the model of the environment, and to allow the human supervisor to select points that define the plane to be disinfected.

The human supervisor then uses a 3D visual interface to specify points bounding the area to be disinfected. We fit a bounded plane to these points, and visualize it in the interface. The human supervisor can interact and move the points around in 3D, until they are satisfied with the position and coverage of the disinfection region. We then use a 2D coverage path planner [29] to generate a trajectory over this plane for the robot end effector, which has a UV-C light source mounted to it, to follow. Using a planar approximation allows us to plan a trajectory in 2D rather than in 6D (3D position and orientation of the robot end effector), greatly simplifying the planning process, without sacrificing coverage (assuming our assumptions of a mostly-planar surface are met). The resulting trajectory and estimated irradiation coverage are then presented to the supervisor for approval, before the robot executes the plan (see Figure 7).

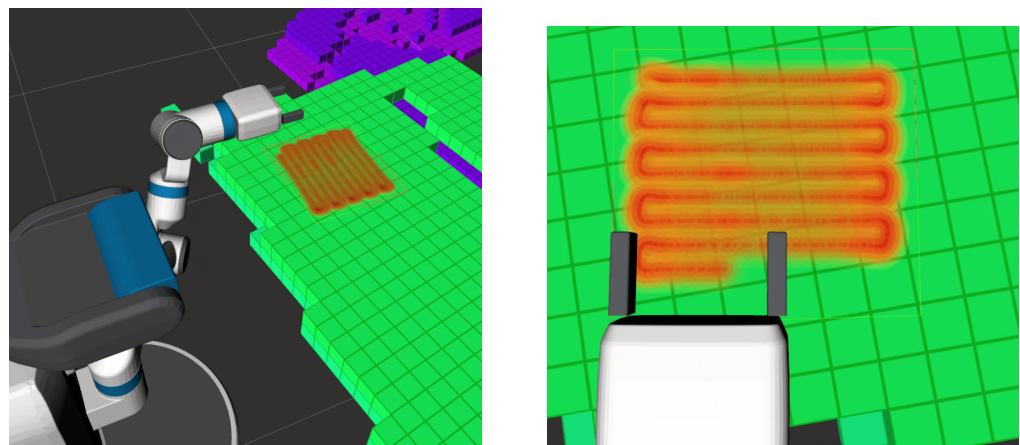


Figure 7. Two views of the heat map visuals.

We developed an empirical model to better estimate the actual irradiation coverage by physically testing the UV dose accumulation from a UV-A light source with a wavelength of 365 nm. Our measuring apparatus comprises 15 Wavshare UV sensor modules [30], that were installed on 3D printed adapters and evenly spaced on a 1 m long aluminum extrusion (see Figure 4). Each sensor was calibrated and capable of measuring UV irradiance values up to 40 mW/cm^2 with a tolerance of $\pm 1 \text{ mW/cm}^2$. The measurement of the delivered UV irradiance was calculated from Equation (2) providing insight that helped develop the empirical model.

Although the propagation of energy in free space is well-understood and could, in theory, be modeled by an inverse square law, our empirical testing revealed deviations from this theoretical model. In particular, as shown in Figures 8 and 9, there is a “shoulder” in the curve, caused by the physical structure of the lights and lenses. Further, Figure 10 shows that the amount of energy received drops over time, presumably as the internal components of the light source heat up and experience a change in internal resistance. To better account for these, we use our best-fit models when calculating the transfer of energy, rather than the (albeit simpler) theoretical model.

Using these models, we calculate the velocity of the robot’s end effector as it follows the planned path to ensure that all areas receive enough irradiation to satisfy the user settings. Three parameters are considered when calculating the end effector velocity: the UV rate constant, k , the disinfection rate, and the UV light distribution of the light source. The disinfection rate and k values are set by the human supervisor in a graphical interface, shown in Figure 11. The UV light distribution is estimated from our empirical models and is assumed to be rotationally invariant. To estimate the amount of irradiation, we discretize the planar surface into cells and move an irradiation mask (see Figure 12).

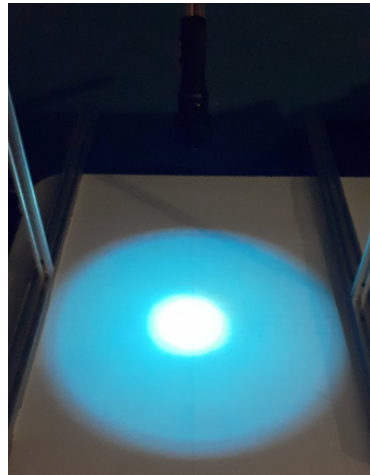


Figure 8. Light distribution from a UV Flashlight. Note that the the center is much brighter than the edges, and that the intensity does not change smoothly with the distance from the center.

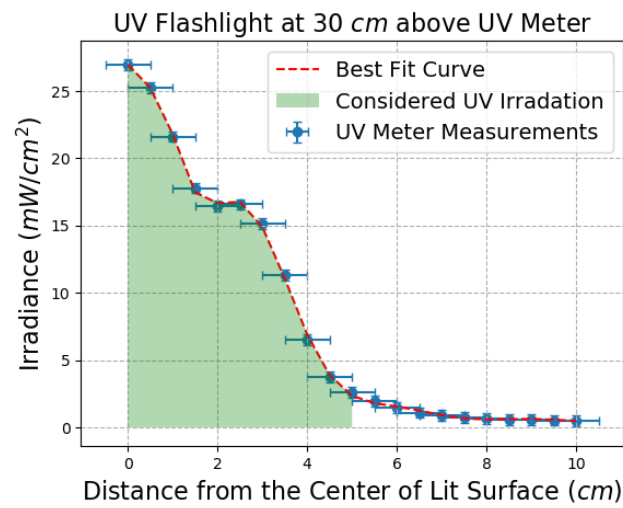


Figure 9. Distance from center vs. Measured Irradiance.

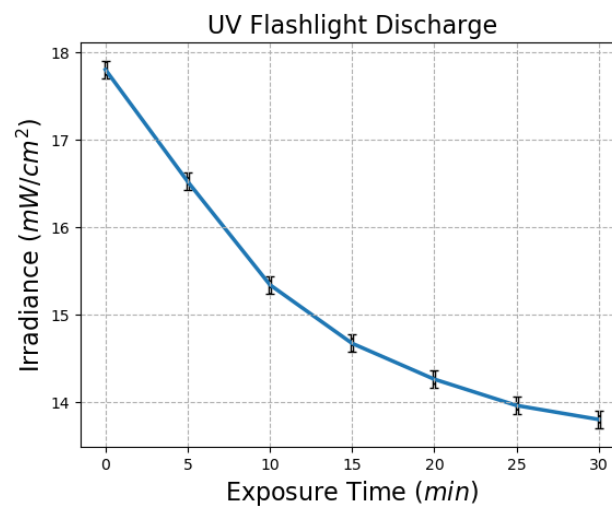


Figure 10. Power drop of UV flashlight as a function of time.

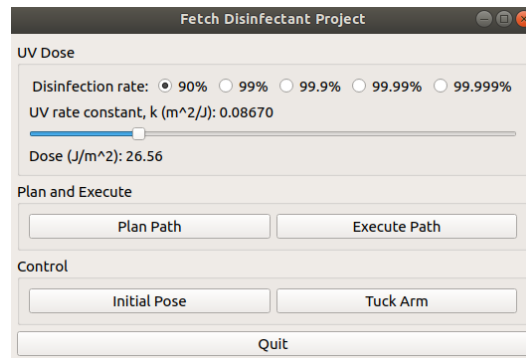


Figure 11. The robot control interface. This allows the user to set the disinfection parameters, and to start the disinfection routine, along with controlling some other basic robot movements.

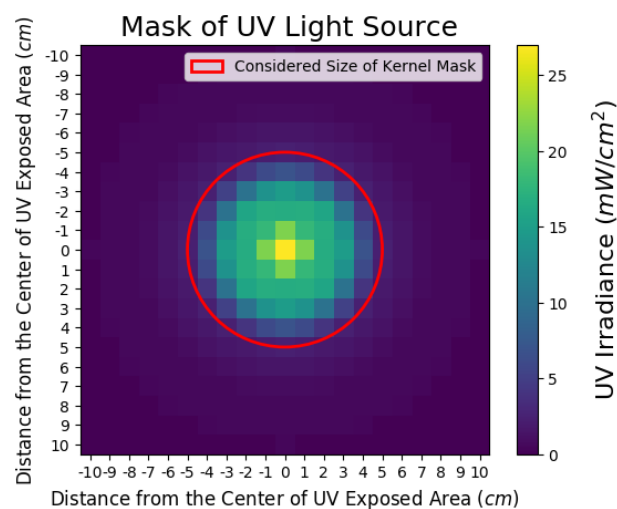


Figure 12. Kernel mask representation of the UV flashlight.

Over it according to the planned trajectory, accumulating irradiation estimates in each of the cells. The end effector trajectory is represented as a sequence of waypoints, and we adjust the velocity between each pair of these waypoints to ensure that sufficient irradiation of the surface, as estimated in our accumulator array, takes place, while attempting to still minimize the total time taken to complete the trajectory.

We tested our system on the parameters of the Ebola Virus Disease, specifically the Sudan strain. The required UV dose for a disinfection rate of 90 percent is 27 J/m^2 . Figure 13 illustrates the accumulated UV irradiance for the 15 sensor array provided by the UV flashlight. Each of the 15 sensors measured past the needed UV dose, verifying the velocity calculation in our path planner to provide adequate UV dose levels for the desired disinfection rate. It is important to note that the manipulator dynamics resulted in a dose saturation at the ends of the sensor array. This behavior makes sense since the manipulator accelerated from zero speed to reach the set velocity. It then decelerated to stop at the last waypoint.

Further technical details of our system and results are available in Sanchez and Smart [31].

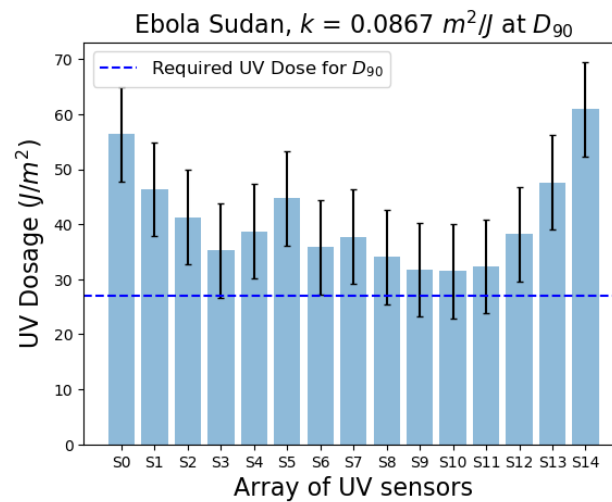


Figure 13. UV Dose measurements for Ebola Sudan at D_{90} .

6. Limitations and Future Work

Our system works well for the disinfection of surfaces, but the current implementation has some limitations. We currently cannot handle surfaces that are larger than the robot's workspace. We currently rely on the human operator to select a surface that the robot can reach all parts of without moving the base. This could be easily addressed for larger areas by cutting the designated surface up into overlapping regions, where each region can be reached from a single location, and then running the planning algorithm for each of them in turn.

Our system also implicitly assumes that the surface is largely flat, with few objects on it. These objects are implicitly assumed to be solid and convex, so that there are no "hidden" surfaces that fall into the shadow of a light above them. While this is, based on our own empirical experience, largely the case of work surfaces, it is an important limitation. While dealing with all possible geometries of objects on the surface would be extremely difficult, it will be relatively straightforward to highlight the areas of the surface that are in shadow from the UV-C light in the graphical interface presented to the user. In the spirit of shared autonomy control, we would then rely on the human supervisor to determine where there are areas that still need disinfection, and to take appropriate action, either with the robot or by tasking a human to complete the job.

Finally, our system assumes a fixed, known calibration for the UV-C light source. However, as our empirical evaluation showed, the output of this light source varied over time. To address this, we plan on installing a UV-C light sensor, as shown in Figure 4, to the robot itself in a known position. This will allow us to periodically check the output of the light and adjust our models to more accurately reflect the current state, leading to more reliable disinfection.

In the Ebola context, disinfecting fomites is the most effective when combating the Ebola virus. However, recent work has shown that fomite transmission is not a significant concern for COVID-19. The most recent results, at the time of writing, suggest that infected respiratory droplets are the primary concern for COVID 19 transmission [32]. This makes a direct application of our system, designed for Ebola, less relevant to the fight against COVID-19 and other similar pathogens where fomite transmission is of lesser concern. In order to make our system more generally applicable, an important next step will be to generalize it to perform open space disinfection.

It is worth noting that Tiseni et al. [23] describe an open-space disinfection system, where a genetic algorithm is used to determine a trajectory that results in an acceptable level of irradiation for a discrete number of points in a room, taken to be representative of the room as a whole. Our proposed future approach is similar in spirit, but aims to model all of the room's free space, not just a discrete set of surface points. Our proposed

approach also allows for more human supervision, making it more adaptable to new spaces, and allowing for humans to “sign off” on the planned disinfection trajectory before it is executed to ensure that it meets their needs.

Our previous work’s general methods can be readily adjusted to open space disinfection. From a technical point of view, the main challenge is moving from a 2D representation (of the surface) to a 3D one (of the open space). The challenge is not one of the representation itself, but in the number of discrete cells that must be considered. For example, for a surface area of one square meter, if we discretize into a grid of cells one square centimeter, we end up with 100,000 cells to consider. If we extend this to one cubic meter with one cubic centimeter cells, we now have 1,000,000 cells. Practically, this means that any computation that considers all of the cells will take (at least) ten times as long and use ten times as much computer memory. To make matters worse, open spaces are generally larger than workspace surfaces, and often considerably so. This greatly exacerbates the problem of larger representations. As a concrete example, the desk at which this author is sitting has an area of approximately 6500 cm². The (normally sized) office in which they are sitting has a volume of approximately 37,280,000 cm³. If an algorithm could determine the UV-C accumulation on the desktop in one second, it would take over an hour and a half to cover the entire room. This means that using the algorithm interactively, as we do now, is not possible for larger spaces without rethinking how we estimate the accumulation of UV-C radiation, perhaps moving away from an exhaustive count in each of the discrete cells into which we divide up the world.

Our approach could easily be used with existing mobile UV disinfection robots such as I-Robot UV-C [33] and UV-Disinfection Robot [34]. In this case, the trajectory that we would plan for the robot is still 2D, representing a sequence of waypoints on the floor. The robot’s velocity between these waypoints could be calculated similarly to our current system. The array that estimates the accumulated irradiation would now be 3D, with most cells representing open space, and we would have to build a new empirical model of propagation. However, the basic underlying approach would carry across straightforwardly.

A more significant change would have to be made in the graphical interface, to allow the user to visualize accumulated irradiation and to specify areas to disinfect. However, the underlying mechanisms of the display would work just as well in the new setting. A facility for manipulating the 3D scene, to look at it from different viewpoints and at different scales would also be necessary, to ensure that all areas of importance receive enough irradiation.

Having the robot move around from place to place would also present uncertainty that is not currently in our system. The exact position of the robot’s end effector is known with considerable accuracy in our current system. The accuracy of the robot’s arm configurations results from having encoders that directly report each joint’s angle and an accurate arm model. We also know the kinematic relationship between the arm and the robot’s sensors. This means that, for any particular sensor reading, we know exactly where it is in the world, with respect to the end effector. However, mobile robots must estimate their position based on sensor information and a map of the world. Localization and pose estimation are inherently inaccurate [35], and these inaccuracies in position will propagate inaccuracies in the estimation of the amount of irradiation delivered to each 3D voxel. To fully capture this stochasticity, it may be necessary to model the amount of irradiation in a given cell not as a scalar value, but as a probability distribution, further increasing the computational cost of the approach.

On a more positive note, such a system could work mostly unattended, once the human supervisor specifies their preferences, and could provide a more continuous, verifiable disinfection of open spaces. Expensive computations could be done overnight and stored for reuse if the large-scale structure of the world does not change much. Finally, the types of calculations to estimate the accumulation of irradiation in the 3D cells are significantly similar to those commonly done when rendering computer graphics scenes, and are well-supported by current video card (GPU) hardware. Implementing these algorithms on a

GPU would lead to significant speed improvements, reducing or eliminating the additional cost incurred by moving to a 3D system.

Author Contributions: Conceptualization, W.D.S.; Data curation, A.G.S.; Investigation, A.G.S. and W.D.S.; Methodology, W.D.S.; Software, A.G.S. and W.D.S.; Validation, A.G.S.; Writing—original draft, A.G.S. and W.D.S.; Writing—review & editing, W.D.S. All authors have read and agreed to the published version of the manuscript.

Funding: This research was funded by the US National Institutes of Health. under number EB024330.

Institutional Review Board Statement: Not applicable.

Informed Consent Statement: Not applicable.

Data Availability Statement: Details regarding our data and Fetch controllabilty package can be found here: https://github.com/osuprg/fetch_disinfectant_project, accessed on 20 December 2021.

Acknowledgments: We would like to thank Zachary Ian Lee for his software support and guidance for this project.

Conflicts of Interest: The authors declare no conflict of interest.

References

1. Nguyen, L.H.; Drew, D.A.; Graham, M.S.; Joshi, A.D.; Guo, C.G.; Ma, W.; Mehta, R.S.; Warner, E.T.; Sikavi, D.R.; Lo, C.H.; et al. Risk of COVID-19 among front-line health-care workers and the general community: A prospective cohort study. *Lancet Public Health* **2020**, *5*, e475–e483. [CrossRef]
2. Gondi, S.; Beckman, A.L.; Deveau, N.; Raja, A.S.; Ranney, M.L.; Popkin, R.; He, S. Personal protective equipment needs in the USA during the COVID-19 pandemic. *Lancet* **2020**, *395*, e90–e91. [CrossRef]
3. Sanchez, A.G.; Smart, W.D. Towards Verifiable COVID-19 Aerosol Disinfection using Ultraviolet Light with a Mobile Robot. In Proceedings of the PETRA 2021: The 14th Pervasive Technologies Related to Assistive Environments Conference, Corfu, Greece, 29 June–2 July 2021; pp. 300–305. [CrossRef]
4. Gelderblom, H.R. Structure and classification of viruses. In *Medical Microbiology*, 4th ed.; University of Texas Medical Branch: Galveston, TX, USA, 1996.
5. Milo, R.; Phillips, R. *Cell Biology by the Numbers*; Garland Science: New York, NY, USA, 2015.
6. Louten, J. Virus Transmission and Epidemiology. 2016. Available online: <https://www.ncbi.nlm.nih.gov/pmc/articles/PMC7148619/> (accessed on 20 December 2021).
7. World Health Organization. What We Know about Transmission of the Ebola Virus among Humans. 2014. Available online: <https://www.who.int/news/item/06-10-2014-what-we-know-about-transmission-of-the-ebola-virus-among-humans> (accessed on 20 December 2021).
8. Potter, A.W.; Gonzalez, J.A.; Xu, X. Ebola Response: Modeling the Risk of Heat Stress from Personal Protective Clothing. *PLoS ONE* **2015**, *10*, e0143461. [CrossRef]
9. Van Doremalen, N.; Bushmaker, T.; Morris, D.H.; Holbrook, M.G.; Gamble, A.; Williamson, B.N.; Tamin, A.; Harcourt, J.L.; Thornburg, N.J.; Gerber, S.I.; et al. Aerosol and surface stability of SARS-CoV-2 as compared with SARS-CoV-1. *N. Engl. J. Med.* **2020**, *382*, 1564–1567. [CrossRef] [PubMed]
10. Kowalski, W. *Ultraviolet Germicidal Irradiation Handbook: UVGI for Air and Surface Disinfection*; Springer Science & Business Media: New York, NY, USA, 2010.
11. Kowalski, W.J.; Bahnfleth, W.P.; Hernandez, M.T. *A Genomic Model for the Prediction of Ultraviolet Inactivation Rate Constants for RNA and DNA Viruses*; International Ultraviolet Association: Boston, MA, USA, 2009; pp. 4–10.
12. Kesavan, J.; Sagripanti, J.L. Disinfection of airborne organisms by ultraviolet C radiation and sunlight. In *Aerosol Science: Technology and Applications*; Wiley: Hoboken, NJ, USA, 2014; pp. 417–439.
13. Nyangaresi, P.O.; Qin, Y.; Chen, G.; Zhang, B.; Lu, Y.; Shen, L. Effects of single and combined UV-LEDs on inactivation and subsequent reactivation of *E. coli* in water disinfection. *Water Res.* **2018**, *147*, 331–341. [CrossRef] [PubMed]
14. King, B.; Kesavan, J.; Sagripanti, J.L. Germicidal UV Sensitivity of Bacteria in Aerosols and on Contaminated Surfaces. *Aerosol Sci. Technol.* **2011**, *45*, 645–653. [CrossRef]
15. Arguelles, P. Estimating UV-C Sterilization Dosage for COVID-19 Pandemic Mitigation Efforts. 2020. Unpublished.
16. Yang, G.Z.; Nelson, B.J.; Murphy, R.R.; Choset, H.; Christensen, H.; Collins, S.H.; Dario, P.; Goldberg, K.; Ikuta, K.; Jacobstein, N.; et al. Combating COVID-19—The Role of Robotics in Managing Public Health and Infectious Diseases. *Sci. Robot.* **2020**, *5*, eabb5589. [CrossRef] [PubMed]
17. Cardona, M.; Cortez, F.; Palacios, A.; Cerros, K. Mobile Robots Application Against COVID-19 Pandemic. In Proceedings of the IEEE ANDESCON, Quito, Ecuador, 13–16 October 2020.
18. Kaiser, M.S.; Al Mamun, S.; Mahmud, M.; Tania, M.H. Healthcare Robots to Combat COVID-19. In *COVID-10: Prediction, Decision-Making, and Its Impacts*; Santosh, K., Joshi, A., Eds.; Springer: Singapore, 2021; pp. 83–97.

19. Di Lallo, A.; Murphy, R.R.; Krieger, A.; Zhu, J.; Taylor, R.H.; Su, H. Medical Robots for Infectious Diseases. *Robot. Autom. Mag.* **2021**, *28*, 18–27. [[CrossRef](#)]
20. Courtney, P.; Royal, P.G. Using Robotics in Laboratories During the COVID-19 Outbreak. *Robot. Autom. Mag.* **2021**, *28*, 28–39. [[CrossRef](#)]
21. Shen, Y.; Guo, D.; Long, F.; Mateos, L.A.; Ding, H.; Xiu, Z.; Hellman, R.B.; King, A.; Chen, S.; Zhang, C.; et al. Robots Under COVID-19 Pandemic: A Comprehensive Survey. *IEEE Access* **2021**, *9*, 1590–1615. [[CrossRef](#)] [[PubMed](#)]
22. Shah, A. Robotic Arms Extend the Reach of UV Disinfection. USC Viterbi School of Engineering Blog Article. 2020. Available online: <https://viterbischool.usc.edu/news/2020/04/robotic-arms-extend-the-reach-of-uv-disinfection/> (accessed on 20 December 2021).
23. Tiseni, L.; Chiaradi, D.; Gabardi, M.; Solazzi, M.; Leonardis, D.; Frisoli, A. UV-C Mobile Robots with Optimized Path Planning. *Robot. Autom. Mag.* **2021**, *28*, 59–70. [[CrossRef](#)]
24. Kraft, K.; Chu, T.; Hansen, P.; Smart, W.D. Real-time Contamination Modeling for Robotic Health Care Support. In Proceedings of the IEEE/RSJ International Conference on Robots and Systems (IROS), Daejeon, Korea, 9–14 October 2016; pp. 2249–2254.
25. Ester, M.; Kriefel, H.P.; Sander, J.; Xu, X. A Density-Based Algorithm for Discovering Clusters in Large Spatial Datasets with Noise. In Proceedings of the Twelfth ACM SIGKDD Conference on Knowledge Discovery and Data Mining (KDD), Philadelphia, PA, USA, 20–23 August 2006; pp. 226–231.
26. Fitzgibbon, A.W.; Pilu, M.; Fisher, R.B. Direct Least Squares Fitting of Ellipses. *IEEE Trans. Pattern Anal. Mach. Intell.* **1999**, *21*, 476–480. [[CrossRef](#)]
27. Judson, S.; Prescott, J.; Munster, V. Understanding Ebola Virus Transmission. *Viruses* **2015**, *7*, 511–521. [[CrossRef](#)] [[PubMed](#)]
28. Mills, D.; Harnish, D.A.; Lawrence, C.; Sandoval-Powers, M.; Heimbuch, B.K. Ultraviolet germicidal irradiation of influenza-contaminated N95 filtering facepiece respirators. *Am. J. Infect. Control* **2018**, *46*, e49–e55. [[CrossRef](#)] [[PubMed](#)]
29. Sakai, A. PythonRobotics. 2021. Available online: <https://github.com/AtsushiSakai/PythonRobotics> (accessed on 20 December 2021).
30. Waveshare. Waveshare: Ultraviolet Sensor. Available online: https://www.waveshare.com/wiki/UV_Sensor (accessed on 20 December 2021).
31. Sanchez, A.G.; Smart, W.D. Surface Disinfection using Ultraviolet Light with a Mobile Manipulation Robot. *arXiv* **2021**, arXiv:cs.RO/2104.10739.
32. World Health Organization. Coronavirus Disease (COVID-19): How Is It Transmitted? 2020. Available online: <https://www.who.int/news-room/q-a-detail/coronavirus-disease-covid-19-how-is-it-transmitted> (accessed on 20 December 2021).
33. Guettari, M.; Gharbi, I.; Hamza, S. UVC disinfection robot. *Environ. Sci. Pollut. Res.* **2020**, *28*, 40394–40399. [[CrossRef](#)] [[PubMed](#)]
34. Rubæk, T.; Cikotic, M.; Falden, S. Evaluation of the UV-Disinfection Robot. 2016. Available online: https://www.gogas.com/images/pdf/health-fakten/gogas_uv_facts_uvdr-whitepaper_004.pdf (accessed on 29 December 2021).
35. Thrun, S.; Burgard, W.; Fox, D.; Arkin, R. *Probabilistic Robotics*; Intelligent Robotics and Autonomous Agents Series; MIT Press: Cambridge, MA, USA, 2005.